Aerodynamic Stall Control of a Generic Airfoil using Synthetic Jet Actuator

Basharat Ali Haider, Naveed Durrani, Nadeem Aizud and Salimuddin Zahir

Abstract—The aerodynamic stall control of a baseline 13-percent thick NASA GA(W)-2 airfoil using a synthetic jet actuator (SJA) is presented in this paper. Unsteady Reynolds-averaged Navier-Stokes equations are solved on a hybrid grid using a commercial software to simulate the effects of a synthetic jet actuator located at 13% of the chord from the leading edge at a Reynolds number Re = 2.1×10^6 and incidence angles from 16 to 22 degrees. The experimental data for the pressure distribution at Re = 3×10^6 and aerodynamic coefficients at Re = 2.1×10^6 (angle of attack varied from -16 to 22 degrees) without SJA is compared with the computational fluid dynamic (CFD) simulation as a baseline validation. A good agreement of the CFD simulations is obtained for aerodynamic coefficients and pressure distribution.

A working SJA has been integrated with the baseline airfoil and initial focus is on the aerodynamic stall control at angles of attack from 16 to 22 degrees. The results show a noticeable improvement in the aerodynamic performance with increase in lift and decrease in drag at these post stall regimes.

Keywords—Active flow control, Aerodynamic stall, Airfoil performance, Synthetic jet actuator.

I. INTRODUCTION

THE aerodynamic performance of any airplane is primarily dependant on its lifting components such as wings. The modern aircraft design uses different high performance airfoils blended in the wing to give the optimized performance. The performance parameters such as the cruise speed, take-off and landing distances, stall speed, handling qualities (especially near the stall, and overall aerodynamic efficiency during all phases of flight [1] are related with the airfoil performance. The airfoil used in this study is a 13-percent thick airfoil derived from the NASA GA(W)-1 airfoil. The airfoil has been designated as General Aviation (Whitcomb)– number two airfoil (GA(W)-2), designed for general aviation applications [2].

Presently, a sizeable aerodynamic community is striving to explore the ways to enhance the aerodynamic performance of the designed airfoils. Some novel techniques such as the synthetic jet actuators are being actively developed as the flow control and stall delay devices. By the application of flow

B. A. Haider is with the National Engineering and Scientific Commission, Islamabad, Pakistan, e-mail: basharatalihaider@yahoo.com.

Dr. N. Durrani is with the National Engineering and Scientific Commission, Islamabad, Pakistan (e-mail: ndurrani@gmail.com).

N. Aizud is with the National Engineering and Scientific Commission, Islamabad, Pakistan.

Dr. S. Zahir is with the National Engineering and Scientific Commission, Islamabad, Pakistan.

control strategies, the airfoil characteristics, such as lift, drag or pitching moment may be optimized without changing angle of attack or flap deflection. Consequently, the active flow control methods may apply to a large variety of problems, e.g. changing lift for rotary wing aircraft [3], achieving lower radar cross-section aircraft, delaying aerodynamic stall to enhance maximum lift [4] or drag reduction.

The initial applications area conceived for the synthetic jet actuator was for the acoustic problems by Ingard [5]. Later, its application to flow control problems was re-discovered and developed by Glezer and co-workers [6] – [9] and Gilarranz [10]. A synthetic jet actuator is a device that alternatively injects and removes fluid through a small orifice at a given frequency, so that the net mass addition to the flow is zero but its net momentum flux is not zero [11].

The working principle of the synthetic jets is very simple. An oscillating piston attached with the flexible membrane also called as the diaphragm generates a fluidic jet. The fluidic jet has a pulsed motion resulting from the alternative suction and blowing through a small orifice segments. At a particular jet Reynolds number, the fluid separates from the orifice lip and results in the formation of a coherent jet into the fluid above it. As pointed in Ref. [12], for sufficiently high amplitudes, a non-symmetric or directed flow is established creating a point source of momentum, with no net mass injection.

The synthetic jet actuators are used to stabilize the boundary layer. The periodic addition/ removal of the momentum flux to/from the boundary layer with the formation of the vertical structures can stabilize the boundary layer. The performance and efficiency of any synthetic jet is greatly dependant on various parameters such as the frequency amplitude, and location of the actuation. An extensive parametric study is necessary for optimizing the control parameters [13].

II. COMPUTATIONAL WORK

The shape of the airfoil used in this study is shown in Fig. 1. The computational grid for aerodynamic stall control on baseline NASA GA(W)-2 airfoil and with the application of synthetic jet actuator is shown in Fig. 2. The low-speed aerodynamic characteristics of this configuration were experimentally performed in Langley low-turbulence pressure tunnel [2] over a Mach number range from 0.10 to 0.35. The chord Reynolds number varied from about 2.0×10^6 to 9.0×10^6. The geometrical angle of attack varied from about -10° to 22°. The pressure distribution of the baseline airfoil is reported in Ref. [2] at Re = 3×10^6.

World Academy of Science, Engineering and Technology
International Journal of Aerospace and Mechanical Engineering
Vol:4, No:9, 2010

The Reynolds number and Mach number selected for controlled and uncontrolled cases are 2.1×10^6 and 0.15 respectively. The flow angle of attack in case of uncontrolled simulation is varied from -10° to 22° for validation while effect of synthetic jet actuator is simulated at 16°, 18°, 20° and 22°, post-stall regime. The pressure distribution is matched with experimental results at a Reynolds number of 3×10^6.
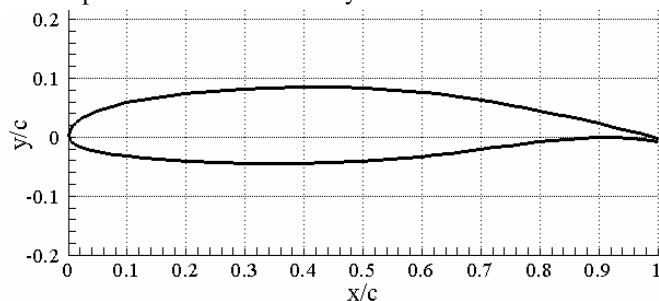

Fig. 1 Shape of NASA GA (W)-2 airfoil

A. Grid Generation

The O-type structured grid is generated on the baseline airfoil of chord length of c = 601 mm. The hybrid grid is generated when synthetic jet actuator is placed at 13% chord location, measured from leading edge. The orifice of SJA has a width of 0.25% of the chord length. The mesh details for both cases are listed in Table I.

TABLE I
MESH STATISTICS OF BASELINE AND CONTROLLED NASA GA (W)-2
AIRFOIL

Case	Type	Cells	Faces	Nodes	y+
Baseline (uncontrolled)	Structured	31360	62944	31584	<1
Controlled (with SJA)	Hybrid	39973	80085	40112	<1

The grid is generated by using a commercial software, "Gridgen". Fig. 2 shows the mesh created for this study. Fig 2(c) shows the unstructured grid inside the synthetic jet actuator with boundary conditions applying to the diaphragm.

B. Flow Solver

The Unsteady Reynolds-Averaged Navier-Stokes (RANS) equations have been solved using a commercial CFD solver "Fluent". The Spalart-Allmaras (S-A) turbulence model is used. The S-A model is effectively a low-Reynolds-number model, requiring the viscous-affected region of the boundary layer to be properly resolved [18].

III. RESULTS AND DISCUSSION

The study is carried out in two steps. Firstly, the pressure distribution (C_p) and aerodynamic coefficients (C_L and C_m) of the baseline airfoil are validated with the available experimental data for a particular Reynolds number. Secondly, the effect of synthetic jet actuator on aerodynamic coefficients is studied. The overall scope of this work involves the determination of the optimized location for the placement of the SJA and then effect of the variation of the oscillation frequency and amplitude. However, the present study as an initial step is limited to find the functional benefit of using the
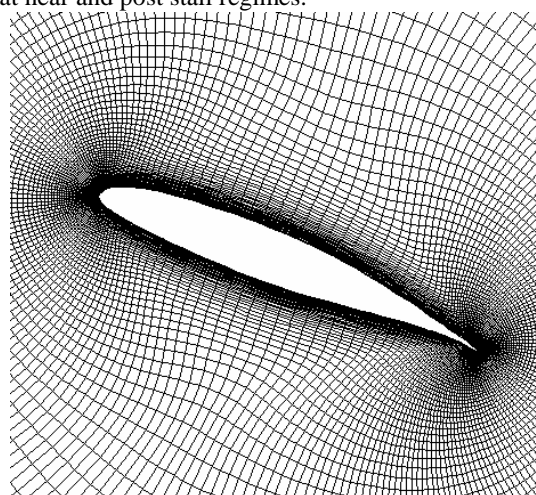
SJA at near and post stall regimes.

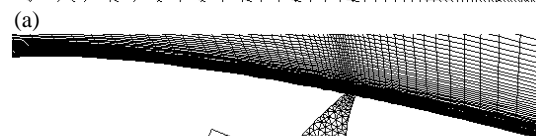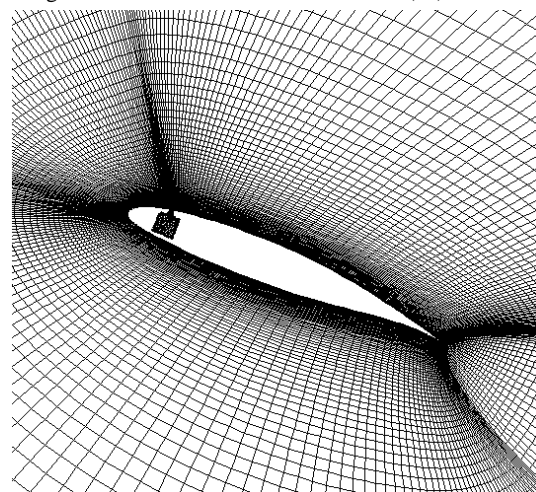Fig. 2 Mesh around baseline NASA GA (W)-2 airfoil

(a)

(b)
Fig. 3 (a) Mesh around controlled NASA GA (W)-2 airfoil with synthetic jet actuator, (b) Unstructured mesh inside the synthetic jet actuator with boundary conditions

A. Pressure Distribution over Baseline Airfoil

The pressure distribution over the baseline airfoil compared with experimental data at four different angles of attack is

World Academy of Science, Engineering and Technology
International Journal of Aerospace and Mechanical Engineering
Vol:4, No:9, 2010

presented in Fig. 4. The CFD results are in a very a good agreement with the experiment.
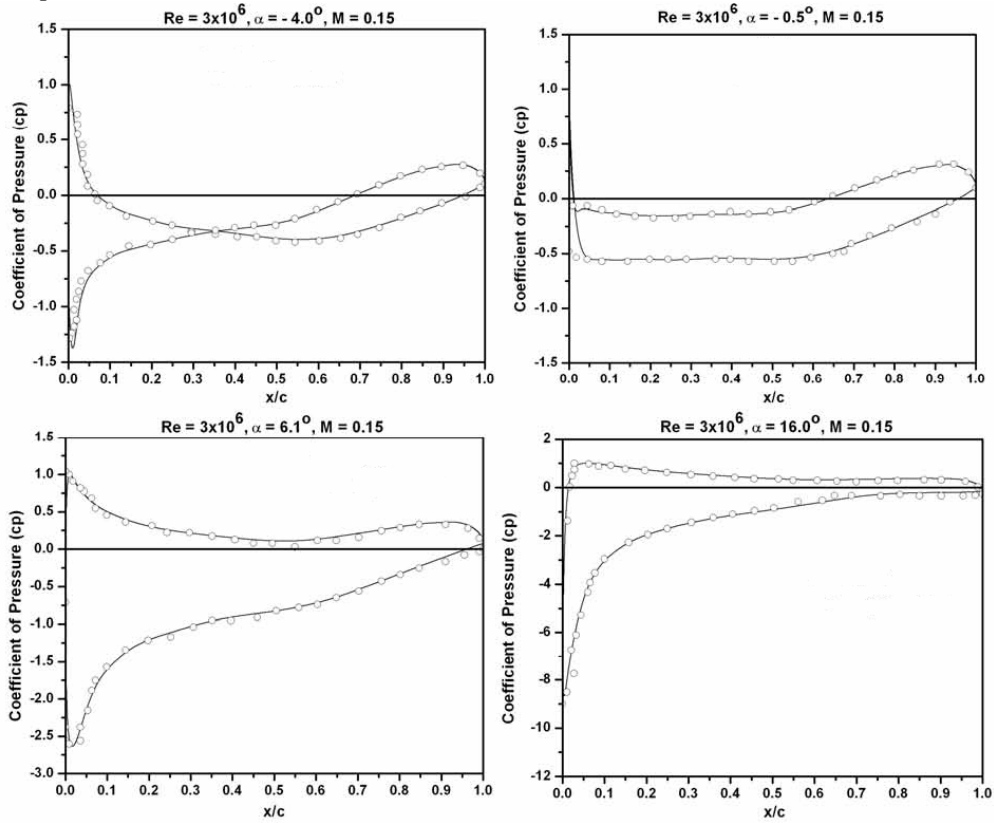
Fig. 4 Pressure distribution over the baseline airfoil at Re = 3x10^6 and M = 0.15 (—, CFD; ○, Experiment)

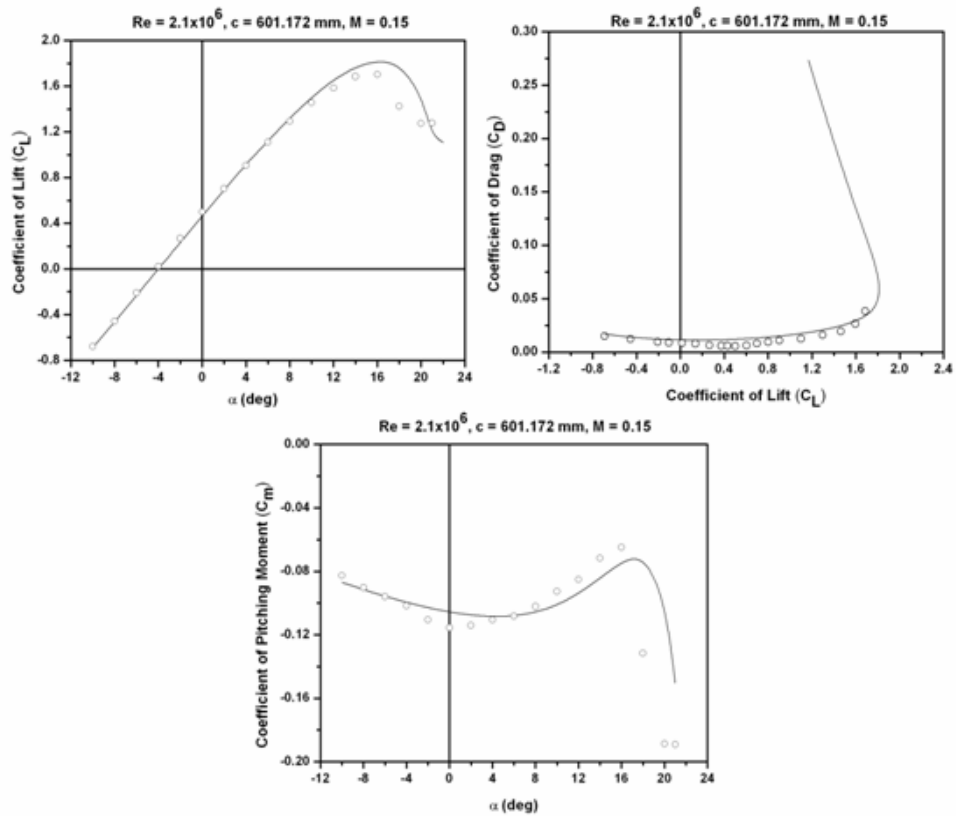Fig. 5 Aerodynamic coefficients of baseline airfoil, comparison of CFD and experiment (—, CFD; ○, Experiment)

World Academy of Science, Engineering and Technology
International Journal of Aerospace and Mechanical Engineering
Vol:4, No:9, 2010

B. Aerodynamic Coefficients of Baseline Airfoil

The lift and pitching moment coefficients of baseline airfoil is presented in Fig. 5, compared with experimental results. The CFD results are predicted well in the linear region while in post-stall regime, a variation in the aerodynamic coefficients is observed, a typical limitation of the RANS.

C. Results of Controlled Airfoil

The momentum coefficient corresponds to each angle of attack is calculated by

$$C_\mu = \frac{h\left(\rho V_{max}^2\right)}{c\left(\rho V_\infty^2\right)} \tag{1}$$

Where h (= 0.0015 m) is the width of the cavity nozzle exit, c (= 0.601 m) is the chord length of the airfoil, V_∞ is the free stream velocity. The V_{max} in (1) corresponds to the maximum velocity at the cavity nozzle exit. The amplitude of oscillations is kept as 0.0012 m with the frequency 217 Hz. A summary of the momentum coefficient at different angle of attacks is shown in Table II.

TABLE II
MOMENTUM COEFFICIENT AT V_∞ = 51.026 AND H = 0.0015 M

α (deg)	V_{max} (m/s)	Momentum Coefficient, C_μ	V_{max}/V_∞
16	113.9365	1.25E-02	2.23
18	89.43551	7.69E-03	1.75
20	114.9407	1.27E-02	2.25
22	120.993	1.41E-02	2.37

The velocity contours in Fig. 6 are presented for the uncontrolled case (without moving the SJA). The contours depict a massive flow separation at the suction side of the baseline airfoil at around 7% of the chord as presented in Fig. 5. The pressure side contours are quite smooth. In the post stall regime, the flow separation at the suction side continues until the downstream wake region. This large separated region leads to a stall adversely affecting the aerodynamic performance of the airfoil. Subsequently, with the introduction of the SJA in the flow, the flow field is presented in Fig. 8-9. Fig. 8 shows the suction segment and Fig. 9 presents the blowing-out segment. The inset of the Fig. 8-9 shows the zoomed view of the flow field. The effect of suction and blowing-out on the near-wall region is clearly observable from these zoomed views. In accordance with its basic principle, the net momentum is added and then removed during the blowing-out and suction cycles respectively causing the flow re-energizing that leads to the stall delay.

The improvement in lift, drag and pitching moment coefficients can be observed in Fig. 10-12. Hence, it can be established that the actuation of the synthetic jet has improved the aerodynamic performance of the baseline airfoil in the post stall regime. The relative gain in lift coefficient at 22 degrees angle of attack predicted by the CFD simulations is more than 30% with reduction in drag about 40%.

IV. CONCLUSION

First part of the paper has been presents good agreement of the pressure distribution with the experimental data. Lift curve

slope is also predicted well in the linear region; with variation in the stall region, a typical limitation of the RANS schemes. A mesh with synthetic jet actuator (SJA) has been generated in "Gridgen" for pre-processing along with the boundary conditions. A user defined function (UDF) is written and integrated with "Fluent" to oscillate the diaphragm as per the required schematic. The results show the working of the SJA is presented in Fig. 10 in a desired fashion. The pressure contours show that the working of SJA with the suction and blowing-out segments. The improvement in the aerodynamic performance in the post stall region as in Fig. 10 and 11 is quite encouraging and it shows that the introduction of SJA is beneficial for the aerodynamics performance of baseline airfoil especially in stall control. As mentioned before, the next step of this study is to explore the placement of the SJA with the optimum performance in the stall control of the baseline airfoil. The effect of change in oscillation frequency and amplitude along with the optimum-performance location will serve as a CFD prediction for the design of SJA with best performance.
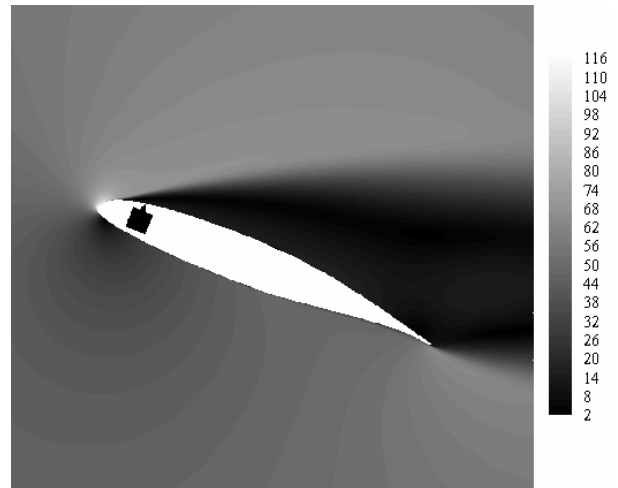

Fig. 6 Contour plots of velocity magnitude (m/s) over an airfoil at angle of attack, α = 22°

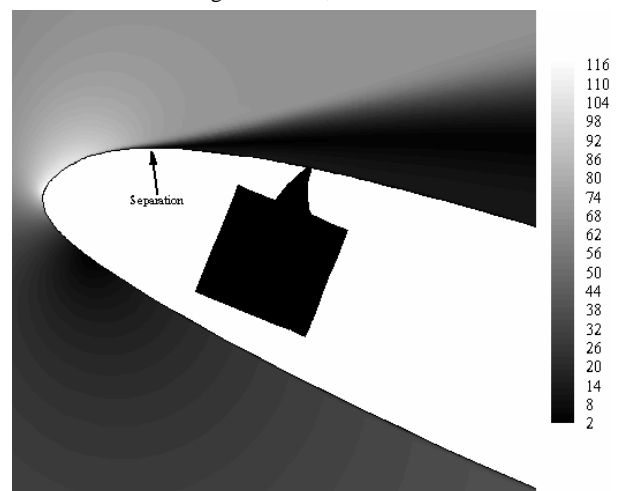Fig. 7 Contour plots of velocity magnitude (m/s) over an airfoil at angle of attack, α = 22°; Flow separation location

World Academy of Science, Engineering and Technology
International Journal of Aerospace and Mechanical Engineering
Vol:4, No:9, 2010

TABLE III
SUMMARY OF AERODYNAMIC COEFFICIENTS

α (deg)	CFD - Controlled Case			CFD - Uncontrolled Case			Experiment - Uncontrolled Case	
	C_L	C_D	C_m	C_L	C_D	C_m	C_L	C_m
16	1.7723	0.0609	-0.0730	1.8246	0.0545	-0.0740	1.7035	-0.0648
18	1.7853	0.0877	-0.0757	1.1097	0.3220	-0.1650	1.4247	-0.1317
20	1.6532	0.1343	-0.0865	1.5338	0.1514	-0.0961	1.2752	-0.1887
22	1.5257	0.1930	-0.1115	1.7994	0.0790	-0.0692	-	

Fig. 8 Contour plots of velocity magnitude (m/s) over an airfoil at
angle of attack, α = 22°, suction segment

Fig. 9 Contour plots of velocity magnitude (m/s) over an airfoil at
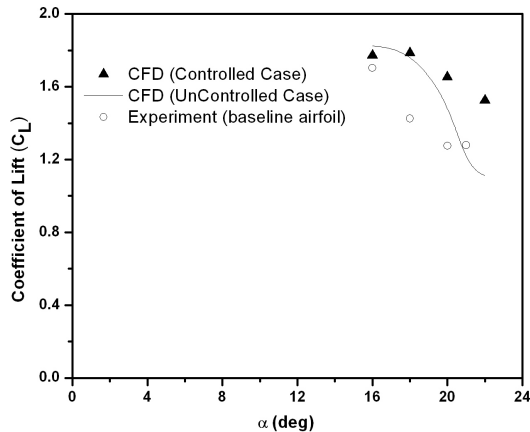angle of attack, α = 22°, blowing-out segment

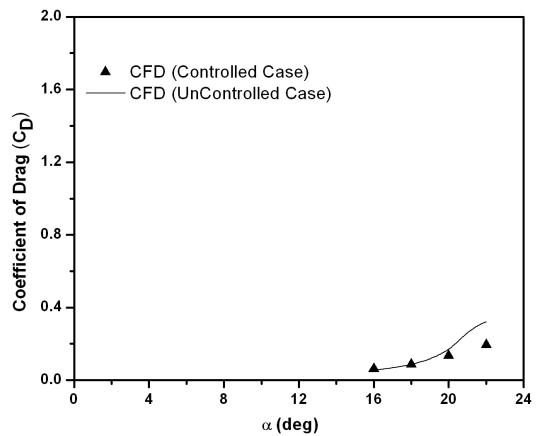Fig. 10 Lift coefficient as a function of angle of attack at Re = 2x10^6
and M = 0.15

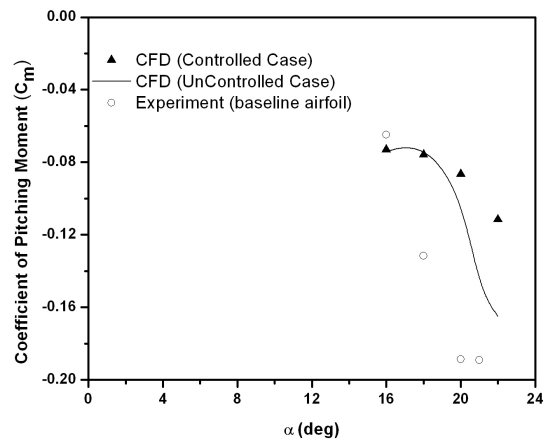Fig. 11 Drag coefficient as a function of angle of attack at Re = 2x10^6
and M = 0.15

Fig. 12 Pitching moment coefficient as a function of angle of attack
at Re = 2x10^6 and M = 0.15

REFERENCES

[1] Daniel P. Raymer, *Aircraft Design: A Conseptual Approach.* 3rd edition. AIAA Education Series, Reston, VA, 1999, pp. 39.
[2] Robert J. McGhee, William D. Beasley, and Dan M. Somers, "Low Speed Aerodynamic Characteristics of a 13-Percent-Thick Airfoil Section designed for General Aviation Applications," NASA TM X-72697, NASA Langley Research Center, Hampton, Virginia.
[3] Hassan A, Straub F, BD C., "Effects of Surface Blowing/Suction on the Aerodynamics of Helicopter Rotor Blade-Vortex Interactions-a Numerical Simulation", Journal of American Helicopter Society 1997,182-194.
[4] Seifert A, Darabi A, Wygnanski I. Delay of airfoil Stall by Periodic Excitation. AIAA Journal, Vol. 33, No. 4, 1996, pp. 691-707.
[5] Ingard, U., "On the Theory and Design of Acoustic Resonators." The Journal of the Acoustical Society of America, Vol. 25, No. 6, 1953, pp. 1037–1060.
[6] Barton L. Smith and Ari Glezer, "The Formationand Evolution of Synthetic jets", Physics of Fluids, vol. 10, No. 9, 1998, pp. 2281-2297.

[7] Smith, B. and Glezer, A., "Jet Vectoring Using Synthetic Jet Actuators," Journal of Fluid Mechanics, Vol. 458, 2002, pp. 1–34.

[8] Amitay, M., Smith, D., Kibens, V., Parekh, A. and Glezer, A., Aerodynamic flow control over an unconventional airfoil using synthetic jet actuators" AIAA Journal, Vol. 39, No. 3, pp. 361-370, March 2001.

[9] Glezer, A. and Amitay, M., "Synthetic Jets," Annual Review of Fluid Mechanics, Vol. 34, 2002, pp. 503–529.

[10] Gilarranz, J. L., Traub, L. W. & Rediniotis, O. K., "A New Class of Synthetic Jet Actuators - Part II: Application to Flow Separation Control," *ASME Journal of Fluids Engineering*, 127, 2005, pp. 377-387.

[11] Omar D. Lopez and Robert D. Moser, "Delayed Detached Eddy Simulation of Flow over an Airfoil", Asociación Argentina de Mecánica Computacional Vol. XXVII, 2008, pp. 3225-3245.

[12] Kevin E. Wu and Kenneth S. Breuer, "Dynamics of Synthetic Jet Actuator Arrays for Flow Control", AIAA, 2003.

[13] D. You and P. Moin, "Study of Flow Separation over an Airfoil with Synthetic Jet Control using Large-Eddy Simulation," Center for Turbulence Research, Annual Research Briefs 2007.

[14] R. Duvigneau and M. Visonneau, "Optimization of a Synthetic Jet Actuator for Aerodynamic Stall Control", *Computers & Fluids*, Vol. 35, No 6, pp 624-638, July 2006

[15] R. Duvigneau and M. Visonneau, "Simulation and Optimization of Stall Control for an Airfoil with a Synthetic Jet," *Aerospace Science & technology*, Vol. 10, No 4, pp 279-287, May 2006

[16] D. You and P. Moin, "Large-Eddy Simulation of Flow Separation over an Airfoil with Synthetic Jet Control," Center for Turbulence Research, Annual Research Briefs 2006.

[17] Guang HONG, "Enabling Micro Synthetic Jet Actuators in Boundary Layer Separation Control Using Flow Instability," *16th Australasian Fluid Mechanics Conference*, Crown Plaza, Gold Coast, Australia, 2007, pp. 887-891.

[18] Fluent User Manual. (www.fluent.com)